

# Organometallic vapor phase epitaxy of GaAs<sub>1-x</sub>N<sub>x</sub> alloy layers on GaAs(001): Nitrogen incorporation and lattice parameter variation

J.-N. Beaudry,<sup>a)</sup> R. A. Masut, and P. Desjardins

*Regroupement québécois sur les matériaux de pointe (RQMP), Département de Génie Physique, École Polytechnique de Montréal, P.O. Box 607, Station Centre-ville, Montréal, Québec H3C 3A7, Canada*

P. Wei, M. Chicoine, G. Bentoumi, R. Leonelli, and F. Schiettekatte

*Regroupement québécois sur les matériaux de pointe (RQMP), Département de Physique, Université de Montréal, P.O. Box 6128 Station Centre-ville, Montréal, Québec H3C 3J7, Canada*

S. Guillon

*Bookham Technology plc, Caswell, Towcester, Northamptonshire NN12 8EQ, United Kingdom*

(Received 12 September 2003; accepted 2 February 2004; published 11 May 2004)

Epitaxial GaAs<sub>1-x</sub>N<sub>x</sub> alloy layers, nominally 200-nm-thick, with  $x$  up to 0.0375 were grown on GaAs(001) at temperatures  $T_s$  varying from 500 to 650 °C to investigate nitrogen incorporation and lattice parameter variations during organometallic vapor phase epitaxy from trimethylgallium, tertiarybutylarsine, and 1,1-dimethylhydrazine. Quantitative secondary ion mass spectrometry measurements (SIMS) indicate that N incorporation decreases systematically with increasing  $T_s$  to become almost negligible at 650 °C. All films are coherent with the substrate as judged by high-resolution x-ray reciprocal lattice mapping although atomic force microscopy and cross-sectional transmission electron microscopy reveal the presence of cracks in films with  $x > 0.02$ . High-resolution x-ray diffraction measurements combined with SIMS analyses indicate that the lattice constant decreases linearly with increasing  $x$  following closely the predictions of Vegard's rule for  $x < 0.03$ . At higher concentrations, the lattice constant decreases more rapidly as a significant fraction of N atoms becomes incorporated in nonsubstitutional sites as demonstrated by nuclear reaction analysis. © 2004 American Vacuum Society. [DOI: 10.1116/1.1689296]

## I. INTRODUCTION

The incorporation of dilute quantities of nitrogen in III-V semiconductors leads to a large reduction of the energy band gap accompanied by a decrease in lattice constant.<sup>1</sup> It has also been demonstrated that the large conduction-band offset in (In)GaAsN/GaAs heterojunctions leads to a better electron confinement and thus an improved temperature stability in heterostructure lasers.<sup>2</sup> These properties make dilute semiconductor nitrides particularly attractive for optical communications at 1.3 and 1.55  $\mu\text{m}$  wavelengths.

There are, however, severe challenges associated with the growth of N-containing III-V semiconductor alloys. First, dilute III-V nitride alloys exhibit a miscibility gap. This argues for epitaxial growth under highly kinetically constrained conditions in order to take advantage of the fact that surface solubilities are orders of magnitude larger than bulk values while simultaneously inhibiting phase separation during deposition. Another obstacle to be overcome is the extremely large difference between the shorter Ga-N covalent bond length compared to those for Ga-As and In-P. Moreover, N atoms, due to their very small covalent radii, could tend to be incorporated on nonsubstitutional lattice sites of the zincblende structure or to form defect complexes.

In order to reduce the lattice parameter and controllably tailor the optoelectronic properties of dilute III-V nitride alloys, it is strongly desirable that N atoms occupy substitu-

tional sites. Zunger and collaborators<sup>3,4</sup> used pseudopotential methods and large atomically relaxed supercells to investigate the effects of short-range ordering and small nitrogen aggregates on the electronic structure and optical properties of III-V-N alloys. However, little is known concerning the detailed N incorporation mechanisms and pathways in III-V semiconductors during epitaxial growth.

The general trends observed in molecular-beam epitaxy and organometallic vapor phase epitaxy (OMVPE) of GaAs<sub>1-x</sub>N<sub>x</sub> on GaAs(001) is that the lattice constant initially decreases linearly with  $x$  up to about 0.015–0.020 at a rate in close agreement with predictions from Vegard's rule. At higher concentrations, however, the lattice constant has been reported to decrease either slower or faster depending on the growth technique or process conditions.<sup>5–7</sup> Recently, it was suggested that differences in stresses measured via wafer curvature measurements and those obtained from high-resolution x-ray diffraction (HR-XRD) analyses were likely the signature of significant bowing of the elastic properties of GaAs<sub>1-x</sub>N<sub>x</sub> alloys with  $x > 0.015$ .<sup>8</sup> Nevertheless, no detailed understanding has yet emerged concerning the atomic configurations of N incorporated in epitaxial GaAs layers.

In this article, we present a systematic investigation of N incorporation in 200-nm-thick OMVPE GaAs<sub>1-x</sub>N<sub>x</sub> films with  $x$  up to 0.0375 for growth temperatures  $T_s$  varying from 500 to 650 °C. Our combined HR-XRD and secondary ion mass spectrometry (SIMS) measurements indicate complete N substitutional incorporation at As sites of the zincblende structure for  $x$  up to about 0.03. At higher concentrations,

<sup>a)</sup>Electronic mail: jean-nicolas.beaudry@polymtl.ca

however, the lattice constant decreases more rapidly than predicted by Vegard's rule while nuclear reaction analysis shows that a significant fraction of N atoms incorporates in nonsubstitutional sites.<sup>9</sup>

## II. EXPERIMENTAL PROCEDURE

GaAs<sub>1-x</sub>N<sub>x</sub> layers, nominally 200-nm-thick, were grown on GaAs(001) in a low-pressure cold-wall OMVPE reactor equipped with a fast-switching run-vent manifold with minimized dead volume<sup>10</sup> using Pd-purified hydrogen as the carrier gas, trimethylgallium (TMGa) as the group-III precursor, and tertiarybutylarsine (TBAs) and 1,1-dimethylhydrazine (DMHy) as group V sources. The reactor pressure was set at 100 Torr with a total flow rate maintained at 3000 sccm. The TMGa partial pressure was fixed at 5.0 mTorr for all GaAs<sub>1-x</sub>N<sub>x</sub> growth experiments. This provides a nominal growth rate of 1 μm h<sup>-1</sup>.

Prior to the growth, the substrates were cleaned in acetone, isopropanol, and deionized water, and then chemically etched in HCl for 2 min. They were then dried with purified N<sub>2</sub> and immediately inserted in the reactor and annealed at 650 °C for 10 min under a TBAs flow to obtain a high-quality GaAs(001) surface. 80-nm-thick GaAs buffer layers were deposited at 650 °C prior to adjusting the substrate temperature  $T_s$  for GaAs<sub>1-x</sub>N<sub>x</sub> growth. The buffer layers serve two purposes. They cover any remaining contamination while simultaneously providing a more uniform distribution of terrace lengths. Following  $T_s$  adjustment, DMHy was added to the gas flow without interrupting the process in order to minimize contamination at the GaAs/GaAsN interface. The  $J_{\text{TBAs}}/J_{\text{TMGa}}$  gas flow ratio was maintained at 24.4 while  $J_V/J_{\text{III}}$  and  $J_{\text{DMHy}}/J_{\text{TBAs}}$  flux ratios up to 510 and 20, respectively, were used. Film growth temperatures  $T_s$  were monitored using a thermocouple inserted in the graphite susceptor and controlled, with proportional band feedback, by varying the power applied to the infrared heater.

Total N concentrations were obtained by SIMS using a Cameca IMS-4F operated with a 10 kV Cs<sup>+</sup> incident beam. Samples were kept at -4.5 kV and the primary current at 30 nA. The signal of the <sup>14</sup>N<sup>69</sup>Ga<sup>-</sup> molecular ion was collected. Quantification, within an experimental uncertainty of ±10%, was carried out by comparison with N-implanted GaAs standards. Quantitative time-of-flight elastic recoil detection (TOF-ERD) measurements using a 50 MeV Cu probe beam were carried out to measure residual C incorporation resulting from organometallic precursor decomposition. The TOF-ERD detector is at a fixed scattering angle of 30° to the beam direction. The timing foil, a 20 μg cm<sup>-2</sup> carbon foil, is located at 12.5 cm from the target. The secondary electrons generated from the C foil are collected by a microchannel plate detector giving the first timing signal. We use a surface barrier detector, located 62 cm from the C foil and subtending a solid angle of 0.18 msr, to measure the energy and the second timing signal.

Lattice constants  $a_{\perp}$  along the growth direction, in plane lattice constants  $a_{\parallel}$ , and residual strains were determined from HR-XRD and high-resolution reciprocal lattice maps

(HR-RLM) around symmetric and asymmetric reflections. The measurements were performed in a Philips high-resolution diffractometer using Cu  $K\alpha_1$  radiation ( $\lambda = 0.154\,059\,7$  nm) from a four-crystal Ge(220) Bartels monochromator which provides an angular divergence <12 arc s with a wavelength spread of  $7 \times 10^{-5}$ .  $\omega$ - $2\theta$  overview scans ( $\omega$  is the angle of incidence and  $\theta$  is the Bragg angle) were obtained with a detector acceptance angle of  $\approx 2^\circ$ . An additional two-crystal Ge(220) analyzer was placed between the sample and the detector to obtain high-resolution (detector acceptance angle  $\approx 12$  arc s) scans. HR-RLMs were generated from successive  $\omega$ - $2\theta$  scans starting at different initial values of  $\omega$ .

Cross-sectional transmission electron microscopy (XTEM) analyses were carried out in a Philips CM30 microscope equipped with a LaB<sub>6</sub> electron source operated at 300 kV. Samples were thinned for XTEM observation by conventional mechanical polishing followed by low-angle (4°) Ar-ion milling at 5 keV in a Gatan precision ion polishing system. The ion beam energy was gradually reduced to 3 keV during the final stages of thinning to minimize sample damage. Film thicknesses were determined from XTEM or Pendellösung interference fringes observed in HR-XRD when possible and otherwise with a combination of SIMS profile and profilometry to measure crater depth. Nuclear reaction analyses (NRA) in a channeling geometry were carried out to determine the nonsubstitutional N fraction. The <sup>14</sup>N( $\alpha, p$ )<sup>17</sup>O endothermic reaction resulting from irradiation with a 3.72 MeV He<sup>2+</sup> beam and producing 1.23 MeV protons was selected to minimize background contributions.<sup>11</sup>

## III. EXPERIMENTAL RESULTS

A series of GaAs<sub>1-x</sub>N<sub>x</sub> epitaxial layers, nominally 200-nm-thick, was grown on GaAs(001) as a function of the element V gas fraction  $X_V = J_{\text{DMHy}}/(J_{\text{TBAs}} + J_{\text{DMHy}})$  at temperatures ranging from 500 to 650 °C. SIMS depth profiles indicate that N concentrations remain constant as a function of depth in all layers studied here, where our highest concentration was  $x = 0.0375$ . Elastic recoil detection measurements also reveal that C incorporation is minimal. Figure 1 is a plot of the N fraction  $x$  in GaAs<sub>1-x</sub>N<sub>x</sub> layers as a function of  $X_V$  and  $T_s$ . The N fraction  $x$  increases monotonically with  $X_V$  at a rate which decreases rapidly with increasing  $T_s$ . This behavior can be better quantified by extracting the slope of the initially linear portion in a  $x$  versus  $J_{\text{DMHy}}/J_{\text{TBAs}}$  plot (see inset in Fig. 1). We find that the N incorporation probability, defined as  $x/(J_{\text{DMHy}}/J_{\text{TBAs}})$ , decreases from 0.0036 at 500 °C to 0.0005 at 600 °C to essentially zero at 650 °C (not shown).

All GaAs<sub>1-x</sub>N<sub>x</sub> layers, irrespective of  $x$  and  $T_s$ , were found to be under tensile strain and fully coherent with their GaAs(001) substrates as judged by HR-XRD and HR-RLM. Figure 2 presents typical HR-XRD  $\omega$ - $2\theta$  scans through the 004 Bragg peak from GaAs<sub>1-x</sub>N<sub>x</sub> layers with  $x = 0.009$  and 0.0375 ( $x$  determined by SIMS). These two compositions were selected to illustrate the two growth regimes observed for layers with  $x$  below and above 0.03. The diffraction curve

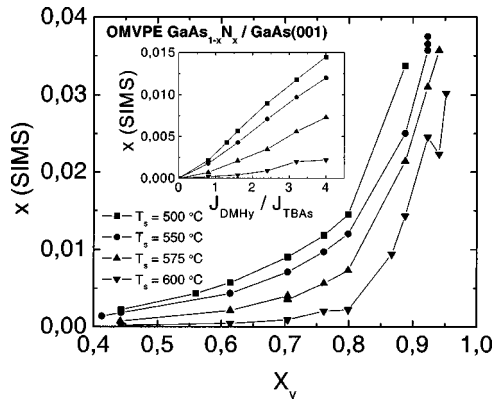


FIG. 1. Incorporated N concentrations  $x$  in OMVPE GaAs<sub>1-x</sub>N<sub>x</sub>(001) layers grown on GaAs(001) as a function of the element V gas fraction  $X_V = J_{DMHy} / (J_{TBAs} + J_{DMHy})$  at temperatures ranging from 500 to 650 °C. The inset shows the N concentration  $x$  as a function of  $J_{DMHy} / J_{TBAs}$ .

for the  $x=0.009$  film grown at  $T_s=500$  °C exhibits a sharp film peak located at +468 arcs with respect to the substrate peak corresponding to a lattice constant  $a_{\perp}$  along the growth direction of 0.56340 nm. The full width at half maximum intensity  $\Gamma_{\omega-2\theta}$  of the film peak in the  $\omega-2\theta$  direction is 100 arc s, essentially equal to the theoretical minimum value, 90 arc s, accounting for strain broadening and finite thickness effects.<sup>12</sup> Interference fringes are clearly visible in Fig. 2 indicating that the alloy layer is of high structural quality with a laterally uniform film/buffer-layer interface. From the fringe spacing, we calculate a layer thickness of 175 nm.

A simulated 004 HR-XRD rocking curve, calculated using the fully dynamical formalism of Tagaki<sup>13</sup> and Taupin<sup>14</sup> is shown in Fig. 2 for comparison. The simulation was carried out using the total N fraction determined by SIMS, assuming perfectly abrupt and coherent interfaces (in agreement with HR-RLM results below), linearly interpolated elastic constants,<sup>15</sup> and the validity of Vegard's rule. The measured and simulated curves are in very good agreement with respect to angular positions of the Bragg peaks and finite-thickness interference fringes. Complementary asymmetric

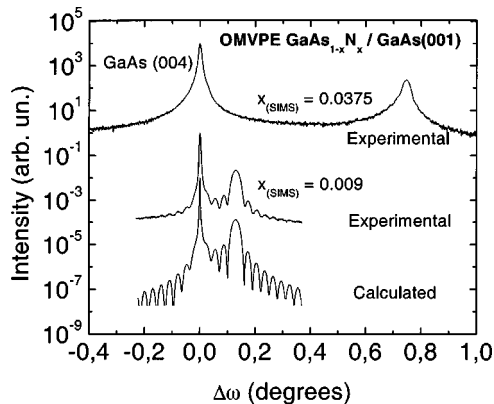


FIG. 2. HR-XRD  $\omega-2\theta$  scans through the 004 Bragg peak from OMVPE GaAs<sub>1-x</sub>N<sub>x</sub> layers with  $x=0.009$  and 0.0375 grown on GaAs(001) at  $T_s=550$  °C. A dynamical simulation is shown for the  $x=0.009$  sample. Curves are shifted vertically for clarity.

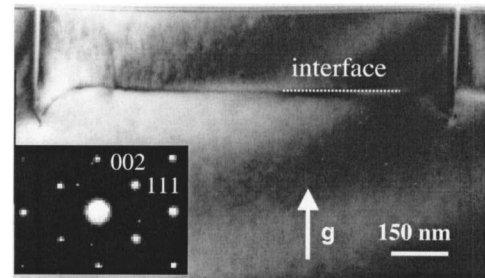
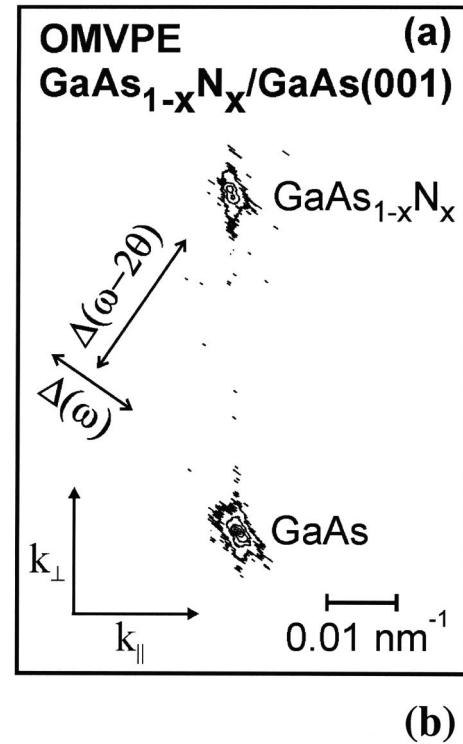


FIG. 3. (a) HR-RLM around the 224 Bragg peak from an OMVPE GaAs<sub>0.9625</sub>N<sub>0.0375</sub> layer grown on GaAs(001) at  $T_s=550$  °C. (b) Bright-field XTEM image, obtained with  $g=002$  near  $[1\bar{1}0]$ , from a GaAs<sub>0.9625</sub>N<sub>0.0375</sub> layer grown on GaAs(001) at  $T_s=550$  °C. A 110 selective area electron diffraction pattern is shown in the inset.

115 HR-XRD scans indicate that the layer is fully coherent with its substrate as expected from the presence of well defined finite-thickness interference fringes in the 004 scan.

An HR-XRD 004  $\omega-2\theta$  scan from a 230-nm-thick GaAs<sub>0.9625</sub>N<sub>0.0375</sub> layer grown at  $T_s=550$  °C is also shown in Fig. 2. The layer peak position is at +2600 arc s with respect to that of the substrate. In this case,  $a_{\perp}=0.5544$  nm.  $\Gamma_{\omega-2\theta}$  is 100 arc s, somewhat larger than the theoretical value of 75 arc s (Ref. 12) and indicative of a decrease in crystalline quality. We attribute the absence of finite-thickness interference fringes, even though the layer is fully coherent as judged by HR-RLM, to the presence of cracks as revealed by XTEM (see below).

A typical HR-RLM around the asymmetric 224 Bragg reflection from the same sample is shown in Fig. 3(a). Diffracted intensity distributions are plotted as iso-intensity contours as a function of the reciprocal lattice vectors parallel  $k_{\parallel}$  and perpendicular  $k_{\perp}$  to the surface. The film and substrate peaks are perfectly aligned along the  $k_{\parallel}$  direction showing

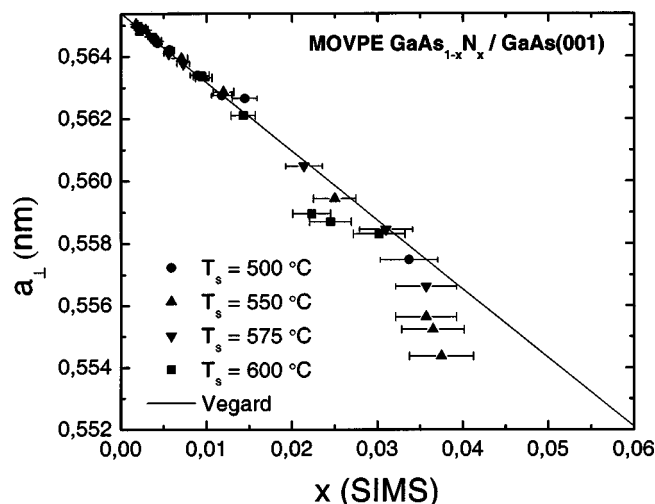


Fig. 4. Lattice parameter  $a_{\perp}$  along the growth direction as a function of the total N concentration  $x$  in 200-nm-thick GaAs<sub>1-x</sub>N<sub>x</sub> layers grown at  $T_s = 500$ – $600$  °C. The solid symbols are experimental results. The solid line corresponds to Vegard's rule.

that the layer is fully coherent with negligible in-plane strain relaxation to within the detection limit of the instrument,  $1 \times 10^{-5}$ . The vertical separation between the film and substrate diffracted intensity distributions corresponds to a tetragonal distortion of  $1.98 \times 10^{-2}$  along the growth direction yielding  $a_{\perp} = 0.5541$  nm, in good agreement with the HR-XRD  $\omega$ - $2\theta$  scan results (0.5544 nm). The full width at half maximum intensity  $\Gamma$  values in the  $\omega$  and  $\omega$ - $2\theta$  directions,  $\Gamma_{\omega}$  and  $\Gamma_{\omega-2\theta}$ , for the film peak are essentially equal to those of the substrate indicating negligible mosaicity.

Even though HR-RLMs indicate that all tensile strain GaAs<sub>1-x</sub>N<sub>x</sub> layers are fully coherent with their GaAs(001) substrates, plan-view Normarski optical microscopy and XTEM reveal the presence of cracks along the  $\langle 110 \rangle$  directions in films with  $x > 0.02$ . Figure 3(b) is a typical bright-field XTEM image, obtained using the  $g = 002$  diffraction near the  $[1\bar{1}0]$  zone axis, from a layer with  $x = 0.0375$ . Cracks extending through the whole film thickness into the substrate and distributed periodically are clearly visible. From observations over more than  $40 \mu\text{m}$  of interface, we determine that their linear density is approximately  $0.8 \mu\text{m}^{-1}$ . In regions between the cracks, the layer is of excellent crystalline quality and its surface is flat to within the resolution of TEM. Strain contrast due to lattice mismatch is noticeable at the interface. No misfit dislocations were visible using bright- and dark-field imaging with  $g = 220$ , confirming that the film/buffer-layer interface is coherent between the cracks as expected from the HR-RLM results presented in Fig. 3. The  $[1\bar{1}0]$  zone axis selected area electron diffraction pattern in the inset consists of single-crystal reflections.

Lattice parameters  $a_{\perp}$  along the growth direction are plotted in Fig. 4 as a function of  $x$  for alloys grown at  $T_s = 500, 550, 575,$  and  $600$  °C. Measured  $a_{\perp}$  values, which are related to the elastic constants  $C_{11}$  and  $C_{12}$  as well as the lattice parameters  $a_{\text{GaAs}}$  and  $a_{\text{GaN}}$  through the relationship  $a_{\perp} = a_{\text{GaAs}} - [(c_{11} + 2c_{12})/c_{11}](a_{\text{GaAs}} - a_{\text{GaN}})x$ , decrease lin-

early with increasing  $x$  following closely the predictions of Vegard's rule (interpolated between GaAs and cubic GaN) for  $x$  up to approximately 0.03. At higher concentrations, however, the lattice constant decreases much more rapidly. Our data also indicate that, although the overall N incorporation probability strongly depends on  $T_s$ , the temperature does not have a marked effect on  $a_{\perp}$  for a given  $x$  value except for films grown at  $600$  °C which exhibit small departures from Vegard's rule from  $x$  of about 0.02. As discussed below, deviations from Vegard's rule in alloys comprising atoms of very different sizes are commonly observed as a result of incorporation on atomic sites leading to a reduction of the overall film strain.<sup>16</sup> This behavior is generally explained by the formation of split interstitials occupying single lattice sites, therefore increasing the lattice constant by an amount similar to the reduction caused by substitutional atoms. In our experiments, however, we observe that  $a_{\perp}$  in alloys with  $x > 0.03$  decreases even more rapidly than for substitutional N incorporation, suggesting that a completely different mechanism is operating. In order to elucidate this behavior, we have directly measured the fraction of nonsubstitutional N atoms by channeling NRA experiments.<sup>9</sup> Results from a GaAs<sub>0.9643</sub>N<sub>0.0357</sub> film reveal that  $\approx 20\%$  of the N atoms occupy nonsubstitutional sites of the zincblende lattice.

#### IV. DISCUSSION

N fractions in GaAs<sub>1-x</sub>N<sub>x</sub>/GaAs(001) layers determined by SIMS as a function of film growth conditions indicate that N incorporation decreases systematically with increasing  $T_s$  to become negligible at  $650$  °C. All films are of excellent quality and fully coherent with their substrate as judged by HR-RLM and XTEM. However, XTEM shows that layers with  $x > 0.02$  contain cracks aligned along the  $\langle 110 \rangle$  directions. The lattice constant in the growth direction,  $a_{\perp}$ , decreases linearly with  $x$  closely following the prediction of Vegard's rule for  $x < 0.03$ . At higher concentrations,  $a_{\perp}$  decreases substantially more rapidly with  $x$ . NRA measurements on a film with  $x = 0.0357$  indicate that approximately 20% of incorporated N atoms occupy nonsubstitutional lattice sites.

A precise experimental determination of how N atoms incorporate in III-V-N dilute alloys for  $x > 0.03$  remains a difficult task since little is known about the energetics and strain coefficients of the possible configurations involving several N, Ga, and As atoms. We also need to determine if the presence of cracks has an impact on lattice constant values obtained from HR-XRD measurements. While they undoubtedly decrease considerably the overall strain energy stored in the substrate-layer system and allow the bent wafer to at least partly recover its initial shape, their effect on HR-XRD measurements should be negligible since, on average, they are more than  $1 \mu\text{m}$  apart (close to the coherence length of the x-ray beam). Moreover, HR-RLMs clearly demonstrate that the layers are coherent with the substrate while XTEM analyses show no evidence of misfit dislocations between the cracks.

The out-of-plane lattice constant  $a_{\perp}$  for fully coherent GaAs<sub>1-x</sub>N<sub>x</sub> layers on GaAs(001) can be expressed as a linear combination of the strains associated with N in each lattice configuration,

$$a_{\perp} = a_{\text{GaAs}}(1 + \alpha_{\text{sub}}x_{\text{sub}} + \bar{\alpha}_{\text{complexes}}x_{\text{complexes}}), \quad (1)$$

where  $x = x_{\text{sub}} + x_{\text{complexes}}$ .  $x_{\text{sub}}$  is the N atom concentration incorporated in substitutional sites of the zincblende lattice while  $x_{\text{complexes}}$  is the N fraction on all other sites.  $\alpha_{\text{sub}}$  represents the lattice distortion in the perpendicular direction (corresponding to the Vegard's rule parameter,  $\alpha = -0.39$ ) while  $\bar{\alpha}_{\text{complexes}}$  corresponds to the average perpendicular strain for nonsubstitutional N. Using the NRA data for the  $x = 0.0357$  film and the measured  $a_{\perp}$  value, we estimate that the average strain associated with these complexes is approximately 2.2 times larger than that for substitutional N.

The fact that the lattice constant for films with  $x > 0.03$  decreases more rapidly than for complete substitutional incorporation would be counterintuitive if minimization of the film strain energy was the primary driving force leading to lattice distortion. Split interstitials occupying a single site of the GaAs lattice can be easily ruled out as they would result in a large compressive strain. In the absence of detailed strain data for the various N configurations in GaAs, we can make a semiquantitative comparison with results for the Ge-C system<sup>16</sup> since Ge has approximately the same lattice parameter as GaAs, a similar lattice structure (diamond instead of zincblende), and the covalent radius of C is relatively close to that of N. The strain coefficient for substitutional C is  $-0.71$  while Ge-C split interstitials have a value of  $\alpha = +0.95$ . We also note that split interstitials typically have large formation energies (several eV) and would not normally be expected to appear during epitaxial growth. C pairs on a single substitutional sites are characterized by a slightly positive strain coefficient while the lowest-energy clusters involving several C atoms introduce negligible strain.

Thus, it appears that, among all possible arrangements that lead to distortions in the lattice, the substitutional N<sub>As</sub> is the one most likely to produce maximum tensile strain in a zincblende lattice. This can only account for perpendicular lattice parameters with values not lower than those predicted by Vegard's law. Our experimental data and analysis suggest that considerations other than strain, such as, for example, the more ionic character of the bond with N addition, have to be taken into account to properly describe the properties of GaAs<sub>1-x</sub>N<sub>x</sub> alloys with  $x > 0.03$ . Finally, we note that changes in the elastic properties of the film appear unlikely to account for the strong deviation from Vegard's rule since not only the elastic coefficients but also their ratio ( $c_{11} + 2c_{12}/c_{11}$ ) would have to change markedly.

## V. CONCLUSION

Epitaxial GaAs<sub>1-x</sub>N<sub>x</sub>/GaAs(001) alloy layers with  $x$  up to 0.0375 were grown at  $T_s = 500-650$  °C by OMVPE. All films, irrespective of  $x$ , are fully coherent with their substrate as judged by HR-XRD and HR-RLM. XTEM reveals the presence of cracks in films with  $x > 0.02$ . The concentration dependence of the lattice constant, together with NRA measurements, indicate that a significant fraction of N atoms occupy nonsubstitutional sites of the zincblende lattice in films with  $x > 0.03$ . The large negative deviation from Vegard's rule in these films cannot be explained by the formation of split interstitials. Our complete set of experimental results suggests that considerations other than strain must be taken into account to properly describe N incorporation in III-V-N semiconductors.

## ACKNOWLEDGMENTS

The authors acknowledge the technical assistance of Joël Bouchard. This work was supported by the Natural Science and Engineering Council of Canada (NSERC) and Canada Research Chair Program. They also acknowledge the generous support of the Rohm and Haas Company concerning the use of the DMHy organometallic precursor.

<sup>1</sup>See, for example, J. W. Ager, III, *Semicond. Sci. Technol.* **17**, 141 (2002), and references therein.

<sup>2</sup>M. Kondow, T. Kitatani, K. Nakahara, and T. Tanaka, *Jpn. J. Appl. Phys., Part 2* **38**, L1355 (1999).

<sup>3</sup>L. Bellaiche and A. Zunger, *Phys. Rev. B* **57**, 4425 (1998).

<sup>4</sup>P. R. C. Kent and Z. Zunger, *Phys. Rev. B* **64**, 115208 (2001).

<sup>5</sup>W. Li, M. Pessa, and J. Likonen, *Appl. Phys. Lett.* **78**, 2864 (2001).

<sup>6</sup>W. J. Fan, S. F. Yoon, T. K. Ng, S. Z. Wang, W. K. Loke, R. Liu, and A. Wee, *Appl. Phys. Lett.* **80**, 4136 (2002).

<sup>7</sup>S. G. Spruytte, C. W. Coldren, J. S. Harris, W. Wampler, P. Krispin, K. Ploog, and M. C. Larson, *J. Appl. Phys.* **89**, 4401 (2001).

<sup>8</sup>R. Reason, W. Ye, X. Weng, G. Obeidi, V. Rothberg, and R. S. Goldman, *Proceedings of the National Center for Photovoltaics and Solar Program Review Meeting*, Denver (2003), p. 708.

<sup>9</sup>P. Wei, M. Chicoine, F. Schiettekatte, J.-N. Beaudry, R. A. Masut, and P. Desjardins, *J. Vac. Sci. Technol. A*, these proceedings.

<sup>10</sup>P. Cova, R. A. Masut, J. F. Currie, A. Bensaada, R. Leonelli, and C. A. Tran, *Can. J. Phys.* **69**, 412 (1991).

<sup>11</sup>P. Wei, S. Tixier, M. Chicoine, S. Francoeur, A. Mascarenhas, T. Tiedje, and F. Schiettekatte, *Nucl. Instrum. Methods Phys. Res. B* (in press).

<sup>12</sup>P. Fewster, *J. Appl. Crystallogr.* **22**, 64 (1989).

<sup>13</sup>S. Takagi, *Acta Crystallogr.* **15**, 1311 (1962).

<sup>14</sup>D. Taupin, *Bull. Soc. Fr. Mineral. Cristallogr.* **87**, 469 (1964).

<sup>15</sup>Elastic constants for GaAs<sub>1-x</sub>N<sub>x</sub> were linearly interpolated between that of cubic GaN ( $c_{11} = 2.82 \times 10^{11}$  Pa,  $c_{12} = 1.59 \times 10^{11}$  Pa) [K. Kim, W. R. L. Lambrecht, and B. Segall, *Phys. Rev. B* **53**, 16310 (1996)] and GaAs ( $c_{11} = 1.19 \times 10^{11}$  Pa,  $c_{12} = 0.538 \times 10^{11}$  Pa) [O. Madelung ed., *Semiconductors—Basic Data*, 2nd ed. (Springer, Berlin, 1996)].

<sup>16</sup>J. G. D'Arcy-Gall, D. Gall, I. Petrov, P. Desjardins, and J. E. Greene, *J. Appl. Phys.* **90**, 3910 (2001).